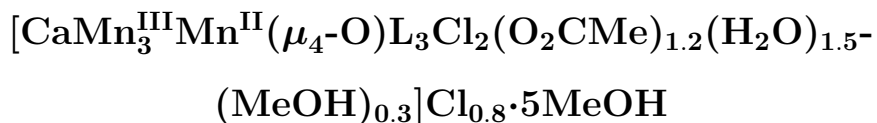


Ab initio study of the magnetic exchange coupling constants of a structural model of the oxygen evolving center in photosystem II:



Heike Fliegl^{a*}, Karin Fink^{a†}, Wim Klopper^{a,b}, Christopher E. Anson^c, Annie K. Powell^{a,c} and Rodolphe Clérac^{d,e}

^a *Institute of Nanotechnology, Forschungszentrum Karlsruhe, P.O. Box 3640, D-76021 Karlsruhe, Germany*

^b *Lehrstuhl für Theoretische Chemie, Institut für Physikalische Chemie, Universität Karlsruhe (TH), D-76128 Karlsruhe, Germany*

^c *Institut für Anorganische Chemie, Universität Karlsruhe (TH), D-76128 Karlsruhe, Germany*

^d *CNRS, UPR 8641, Centre de Recherche Paul Pascal (CRPP) Equipe "Matériaux Moléculaires Magnétiques" 115 avenue du Dr. Albert Schweitzer, Pessac, F-33600, France*

^e *Université de Bordeaux, UPR 8641, Pessac, F-33600, France*

(Dated: October 31, 2008)

* Email: Heike.Fliegl@int.fzk.de

† Email: Karin.Fink@int.fzk.de

Abstract

A new structural model for the oxygen evolving center in photosystem II was recently synthesized and characterized by Hewitt *et al.* [Chem. Commun. **2006**, 2650]. A simplified Heisenberg model Hamiltonian with only two independent constants was applied to extract the magnetic spin-coupling constants J_{ij} of the mixed valent Mn_4 system. In the present study, all six possible coupling constants are calculated by *ab initio* methods in order to obtain a detailed understanding of the magnetic behavior of the system. The broken symmetry approach of Noodleman is applied using density functional theory (DFT). Two different approaches are compared. On the one hand, the coupling constants are obtained from calculations on eight different determinants which describe the high-spin state as well as different broken-symmetry states of the tetranuclear cluster. On the other hand, a pair approach that permits a direct calculation of the individual coupling constants is used. For the pair approach, the coupling constants are also obtained from modified CASCI (Complete Active Space Configuration Interaction) calculations. With the different sets of coupling constants, the full Heisenberg Hamiltonian of the four center problem is used to calculate the magnetic susceptibilities, which are then compared with the experimental values.

I. INTRODUCTION

In nature, the photo-induced oxidation of water to dioxygen $2\text{H}_2\text{O} \rightarrow \text{O}_2 + 4\text{e}^- + 4\text{H}^+$ is efficiently catalyzed by a manganese/calcium complex (Mn_4Ca), which is part of the multi-protein photosystem II (PS II) assembly.[1] Already in 1970, Kok and coworkers[2] proposed a possible mechanism for the water-splitting reaction, cycling the manganese atoms through different oxidation states S_i ($i = 0, 1, 2, 3$ or 4). However, the mechanism of the water-splitting reaction and the structure of the oxygen evolving center (OEC) of PS II are still under debate.[3–5] Regarding the literature, neither the structure of the OEC nor the oxidation states of the four manganese atoms in the different S_i states of the Kok cycle are absolutely clear.

A serious problem lies in the identification of the structure of the reactive center. X-ray absorption spectroscopy (XAS) has been applied successfully, but the interference with the protein environment of PS II and possible damage to the structure by high-energy radiation make a clear assignment difficult. A detailed investigation of a small model cluster, where the structure and the oxidation states of the manganese atoms are well known, could assist in understanding the spectra of the native system and help to identify the several possible oxidation states of the manganese atoms in the different S_i states of the Kok cycle. Investigating the magnetism of such a small model system could also give insight into the question whether magnetic properties play an important role in the catalytic process or not.

In 2006, Hewitt *et al.*[6] succeeded to synthesize a set of model clusters, following the cubane-like structural motive that was proposed by Ferreira *et al.*[3] One of these model clusters, $[\text{CaMn}_3^{\text{III}}\text{Mn}^{\text{II}}(\mu_4\text{-O})\text{L}_3\text{Cl}_2(\text{O}_2\text{CMe})_{1.2}(\text{H}_2\text{O})_{1.5}\text{-}(\text{MeOH})_{0.3}]\text{Cl}_{0.8}\cdot 5\text{MeOH}$ (structure 1 of Ref.6, see Figure 1) serves as a possible model for the S_0 Kok state and yields a $S = \frac{1}{2}$ ground state, which is in nice agreement with an EPR study of Messinger *et al.*[7] L denotes a Schiff-base ligand, which is obtained from the condensation of o-vanillin and 2-hydroxypropylamine. An investigation of the magnetic behavior of this model system was performed using a simplified model Heisenberg Hamiltonian, in which the values of the six possible coupling constants J_{ij} of the Mn_4 system were restricted by the approximations visualized in Figure 2 to avoid overparametrization in the fitting procedure.[6] First, according to the literature[6], the coupling through the central oxygen atom was considered to be negligible, thus J_{12} and J_{23} were set to zero. Second, the coupling between similarly bridged

centers was considered to be identical, therefore J_{14} , J_{24} , and J_{34} were restricted to the same value. Finally, the coupling between the Mn centers 1 and 3 by the CH_3COO^- group was considered to be large and antiferromagnetic ($J_{13} < 0$).

In the present work, we investigate whether these approximations can be justified by *ab initio* calculations. There are in general two approaches to obtain exchange coupling constants by quantum chemical calculations.

On the one hand, the different electronic states of the system can be directly calculated by multi-reference wavefunction-based methods. With these methods, dynamic electron correlation effects can be included and the calculated wavefunctions are eigenfunctions of the Hamiltonian of the molecule as well as of \hat{S}^2 . Unfortunately, applications of multi-reference based methods are restricted to relatively small systems.[8] They are not applicable to a system such as the present Mn_4Ca cluster because the effort increases exponentially with the number of magnetic centers. A way out of this problem may be the pairwise calculation of J values, however. As has been shown by Illas and coworkers,[9] for example, the coupling constants of a system with more than two centers can be obtained from independent calculations on systems with two magnetic centers.

On the other hand, density functional theory (DFT) using the broken symmetry (BS) approach of Noodleman [10, 11] is widely used to obtain coupling constants. This method can be used on relatively large systems. A recent example is the treatment of a Mn_{19} cluster by Ruiz *et al.*[12] In the DFT-BS approach, the high-spin Kohn–Sham (KS) determinant is usually well described, and the exchange coupling constants can be obtained from the difference between the energy of the high-spin state and the energy of broken-symmetry KS determinants, in which the spins of the localized magnetic orbitals [13] are changed from α to β on some of the centers.

Unfortunately, this Noodleman treatment must be regarded with care, since the broken symmetry KS determinants are in general not eigenfunctions of \hat{S}^2 . For a detailed discussion on the proper use of DFT for the extraction of exchange coupling constants, see for instance Refs.14–16 . Alternatively, the constrained DFT approach[16, 17] can be applied, which directly derives the Ising configurations of the system from the density response.

The BS approach has successfully been used in such cases where the local electronic states at the metal centers are spatially nondegenerate. In other cases, it can be necessary to include spin–orbit coupling into the calculations.[18, 19] Mn^{3+} is a d^4 system and in O_h symmetry the

ground state would be a ${}^4T_{2g}$ state. This state is split by the surrounding external ligand field. We have performed Complete-Active-Space Self-Consistent-Field (CASSCF) calculations on mononuclear model complexes to assure that the local ground state can be described by a single determinant and spin-orbit coupling has not to be taken into account. In the present study, the BS approach of Noodlemann is applied using DFT and the Ising approximation, which is considered to provide a reasonable mapping [20, 21] onto the Heisenberg model. The investigation of the magnetic behavior of the model system is extended to the calculation of all six possible exchange coupling constants. In addition, a pair approach that permits a direct calculation of J_{ij} is applied, and furthermore, the coupling constants are obtained by modified Complete-Active-Space Configuration-Interaction (CASCI) calculations [19] for the pair approach. Both approaches are directly compared with experimental values for the magnetic susceptibilities, which are computationally accessible through a Boltzmann average.[13] Finally, a fitting procedure was performed, using the conjugate-gradient method of Polak-Ribiere.[22] The *ab initio* J_{ij} values were taken as the starting points for the minimization procedure, leading so far to the best available estimates of the couplings of the present system.

II. THEORY

A. Exchange coupling constants

The Heisenberg-Dirac-Van-Vleck (HDV) Hamiltonian is defined as

$$\hat{H}^{\text{HDV}} = -2 \sum_{i < j}^N J_{ij} \hat{\mathbf{S}}_i \cdot \hat{\mathbf{S}}_j, \quad (1)$$

where N denotes the number of different local spin centers i with the spin operator $\hat{\mathbf{S}}_i$. J_{ij} is the magnetic spin-coupling constant between the spin centers i and j . J_{ij} is positive for ferromagnetic and negative for antiferromagnetic coupling. The HDV Hamiltonian is widely used to describe the magnetic properties of molecules as well as solids. As soon as the coupling constants are known, the magnetic properties of the system can be determined as shown in the next section. The objective of the present work is to obtain the values for J_{ij} by quantum chemical calculations. The straightforward solution would be to calculate the low-lying electronic states of the molecule and to determine those values of J_{ij} for which

the correct energy levels of the complex are generated by the HDV Hamiltonian. Such a procedure is often used for binuclear complexes, but at present it is not applicable for title compound, because the eigenfunctions of this molecule are multi-reference wavefunctions. In the present work, this procedure based on multi-reference wavefunctions is only used to obtain J values at the CASCI level for *binuclear model* complexes.

As used in the broken symmetry approach of Noodleman [10, 11] and justified by Illas and coworkers,[20, 21] the energy eigenvalue spectrum of the HDV Hamiltonian can be approximated by coupling constants obtained with the Ising Hamiltonian,

$$\hat{H}^{\text{Ising}} = -2 \sum_{i < j}^N J_{ij} \hat{S}_{z,i} \hat{S}_{z,j}. \quad (2)$$

Compared to the HDV Hamiltonian, this is a replacement of the spin operator $\hat{\mathbf{S}}_i$ by its z -component $\hat{S}_{z,i}$. Assuming orthogonality, the high-spin configuration Φ^{HS} , in which all unpaired electrons possess α spin, as well as the broken-symmetry states Φ^{BS} , in which the spins of all unpaired electrons at selected magnetic centers are changed from α spin to β spin, are eigenfunctions of the Ising Hamiltonian.

Since the eigenvalue of the $\hat{S}_{z,i}$ operator with one of the Φ^{BS} states is given by

$$\hat{S}_{z,i} |\Phi^{\text{BS}}\rangle = \pm S_i |\Phi^{\text{BS}}\rangle, \quad (3)$$

the eigenvalues of the Ising Hamiltonian,

$$\hat{H}^{\text{Ising}} |\Phi_i^{\text{BS}}\rangle = E^{\text{BS}} |\Phi_i^{\text{BS}}\rangle, \quad (4)$$

can easily be evaluated from the J_{ij} values.

In the present case, eight different spin states have to be taken into account to obtain the exchange coupling constants. The states as well as their eigenvalues in terms of J_{ij} are listed in Table I. The investigated cluster is a mixed valent Mn_4 system, which contains three Mn^{3+} (d^4) center (labeled with numbers 1–3) with total spin $S = 2$ and one Mn^{2+} (d^5) center with $S = \frac{5}{2}$ (labeled with number 4). The energies E_1 – E_8 are computationally obtained at the DFT level and the magnetic coupling constants J_{ij} are calculated by a least-squares fit to the equations of Table I.

Alternatively, we perform DFT calculations on model clusters with only two magnetic centers. The coupling constants between two interacting centers with identical spins ($S_1 =$

S_2) can directly be calculated with the original Noodlemann formula[10]

$$J_{12} = \frac{E^{\text{BS}} - E(S_1 + S_2)}{S_{\text{max}}^2}, \quad (5)$$

where E^{BS} denotes the energy of the broken-symmetry KS determinant. The high-spin energy is given as $E(S_1 + S_2)$ and the maximum spin of the system is S_{max} . In the present case, a mixed valent Mn system is investigated. Therefore, the two-center problem with identical spins has to be extended to two different spin centers. For the case $S_1 \neq S_2$ the formula[16, 23, 24]

$$J_{12} = \frac{E^{\text{BS}} - E(S_1 + S_2)}{4S_1S_2} \quad (6)$$

is used.

B. Magnetic susceptibilities

Once the exchange coupling constants J_{ij} are known, the full HDV Hamiltonian can be set up according to Eq. (1). The isotropic Zeeman interaction with the external magnetic field B is taken into account by adding the term

$$\hat{H}_Z(B) = \sum_i^N \mu B g_i m_{s_i} \quad (7)$$

to the HDV operator

$$\hat{H}(B) = \hat{H}^{\text{HDV}} + \hat{H}_Z(B). \quad (8)$$

μ denotes Bohr's magneton

$$\mu = \frac{e\hbar}{2m}, \quad (9)$$

where m is the electronic mass and g_i is the effective g factor of center i , which can significantly deviate from the electronic g factor ($g_e=2.0023$) due to spin-orbit coupling. For Mn^{2+} , $g_e=2.0023$ is used, whereas $g = 1.94$ is chosen for the Mn^{3+} centers.[6] The energy eigenvalues of the HDV operator are now accessible via

$$\hat{H}(B)\Phi(S, M_s) = E(B)\Phi(S, M_s) \quad (10)$$

with respect to all possible spin states $\Phi(S, M_s)$ by diagonalizing $\hat{H}(B)$. Then, the magnetic susceptibility $\chi(T)$ as a function of the temperature T can be evaluated from the Boltzmann

average

$$\chi(T) = \mu_0 \frac{M}{B} = -\mu_0 \frac{N_A \sum_{i=1}^n (E_i(B) - E_i(B=0)) \exp(-\frac{E_i(B)}{kT})}{\sum_{i=1}^n \exp(-\frac{E_i(B)}{kT})} \quad (11)$$

over all n possible spin states.[13] N_A denotes Avogadro's number, M is the macroscopic molar magnetization and μ_0 is the vacuum permeability. In this manner, a direct comparison with experimentally measured susceptibilities is possible.

III. COMPUTATIONAL DETAILS

All DFT calculations were performed with the Turbomole program package.[25] The structure was optimized with the BP86 functional [26, 27] of Becke and Perdew, using the def2-TZVP basis set of Weigend *et al.*[28] The magnetic spin-coupling constants were calculated at the B3LYP[29]/def2-TZVP level, since the use of the hybrid B3LYP functional has been shown to be a good choice for the calculation of exchange coupling constants.[30–34] For all calculations, the resolution of the identity approximation (RI) [35–37] was applied.

For the calculation of the magnetic susceptibilities according to Eqs. (7)–(11) a Fortran program by Staemmler *et al.*[38, 39] was generalized to an N -center problem. Applications on complexes with four and more magnetic centers are possible, but note that the number of spin states that have to be considered increases exponentially with the number of involved metal centers. Future applications will be limited to a relatively small number of centers. For the fitting procedure of the *ab initio* coupling constants to experimental susceptibilities, the conjugate gradient method of Polak–Ribiere was applied.[22]

The CASSCF calculations were performed with the Bochum package of *ab initio* programs.[40, 41] We used Huzinaga basis sets [42] for the main group elements. For the atoms which are nearest neighbors to the magnetic centers, we used an $11s7p$ basis set contracted to $7s5p$ and extended by a d -function (exponents, N: 1.0, O: 1.2). The other main group atoms were described by a DZ basis set without further polarization functions. The Mn centers were equipped by a Wachters $15s9p5d$ basis set [43] contracted to $6s4p3d$. An internal contraction was used for the Mn s and p orbitals. In general, all $3d$ orbitals at the Mn centers were considered as active space in the CASSCF calculations. For the mononuclear model clusters, we always performed state-averaged CASSCF calculations, for the binuclear clusters, different schemes were used.

IV. RESULTS

A. Molecular structure

A comparison between the Mn-Mn distances and angles of the optimized structure with the X-ray diffraction (XRD) data is given in Table II. It shows that the DFT optimized Mn₄ cage differs in particular for the Mn₁-Mn₂ and Mn₁-Mn₃ distances from the XRD structure, with deviations about 9 and 8 pm respectively, while almost no difference is observed for the angles. The enlargement of the Mn-Mn distances can be explained with the formation of a hydrogen bond between a water group and a bridging oxygen atom (O₉₅, see Table III) of the CH₃COO⁻ group that connects the Mn₁ and Mn₃ centers. The Mn₃-O₉₅ distance changes about 15 pm and the H-O distance of the hydrogen bridge is 175 pm, which lies in the typical range (≈ 180 pm) for hydrogen bonds.

It is possible that the observed change in the distances determines a change in the occupation of the manganese centers, in particular at the Mn₃ center, whose coordination sphere has mostly been changed. Therefore, CASSCF calculations were performed on a small model system, which is depicted in Figure 3. In the model system, only the first coordination sphere around the Mn₃ center is included and the cluster is saturated by hydrogen atoms. A comparison between the CASSCF results for a model system based on the XRD Mn-O, Mn-Cl and Mn-N bond distances and a second model based on the optimized structure indicates that for the Mn₃ center no changes in the occupation due to the change in the Mn-O distance are observed. The Cl-Mn-O axis has been identified as the Jahn-Teller distortion axis. In the ground state, the e_g type orbital perpendicular to this axis is unoccupied.

For all three Mn³⁺ systems, a significant splitting of the low lying electronic states is observed as can be seen in Table IV. The orbital occupation of the tetranuclear cluster should therefore be unambiguous.

Since the calculated exchange coupling constants are strongly affected by geometrical changes (cf. Tables V and VI), the results based on the XRD structure are considered to be more realistic and are used for the interpretation of the magnetic properties of the title compound.

B. Spin-coupling constants

First, we present the coupling constants obtained from fitting six constants to the eight energies given in Table I. A comparison between the calculated exchange coupling constants for the optimized and the XRD structures is given in Table V. The results for the optimized geometry are found to be smaller than for the XRD structure. Exception are J_{23} and J_{24} , where the situation is reversed. The results for J_{24} are almost identical and the difference between the J_{23} values is small (1.6 K). The largest deviations with 6 and 3 K are found for J_{13} and J_{14} , which are due to the observed geometrical changes of the Mn cluster core, in particular between the Mn_1 and Mn_3 centers.

The calculations indicate that the neglect of the couplings through the central oxygen atom ($J_{12} \approx J_{23} \approx 0$), is not justified. These couplings are identified to be nonidentical and ferromagnetic. For the XRD structure, the calculations confirm that the coupling between the center Mn_1 and Mn_3 through the CH_3COO^- group is indeed the largest antiferromagnetic coupling constant of the whole system. Although the calculations do not confirm that the coupling constants J_{14} , J_{24} and J_{34} are identical (≈ -5 K), the results show that they are all in the same range between -5.7 and -7.5 K.

The absolute values of the antiferromagnetic coupling constants for the XRD structure are in all cases larger than those estimated from experiment, while except for J_{24} , the opposite trend is seen for the J 's for the optimized structure. However, for both structures, all calculated values are in the range suggested by the fit to the experimental data.

In the next step, we investigate whether the observed exchange is dominated by the interaction between directly neighboring Mn centers. Therefore, the exchange coupling constants of every two manganese pairs were calculated in a pair approximation by replacing the other manganese centers of the complex with Al^{3+} for Mn^{3+} and Mg^{2+} for Mn^{2+} , which do not contribute to the coupling, since they provide a closed-shell Ne-like core.

The results of the two center interactions are summarized in Table VI. Although replacing the non-direct neighbors by aluminium and magnesium the same trends as for the complete manganese system are observed for the coupling constants based on the optimized and XRD structures. The comparison to the results based on the XRD structure show that the results of the two-center interactions are very similar (± 0.6 K) to those obtained for the tetranuclear cluster. Exceptions are J_{13} and J_{14} . Here, the calculated results differ with

+1.5 K and -2.3 K from those where all Mn atoms are included.

In the third step, we construct binuclear model complexes which contain only two of the magnetic ions, their nearest neighbors saturated with hydrogen atoms, and the bridging units. Then we calculate the coupling constants with the modified CASCI method as described in Ref. 19. For the systems with one Mn(III) and one Mn(II) center, we perform a state-averaged CASSCF calculation for all five low lying decet states, in which four electrons are localized at the Mn(III) center and five electrons at the Mn(II) center (neutral configurations). The partly occupied orbitals are transformed into localized magnetic orbitals by a Foster–Boys localization procedure[44] We perform a Valence Configuration Interaction calculation (VCI) in the space of these orbitals for states with $m_s = 3.5$ and obtain J_{VCI} from the energy difference of the lowest octet and decet state. These two states were well separated in energy. J_f is obtained from a CI calculation in the subspace of the neutral configurations. The energies of the charge-transfer states, which are important for the super-exchange coupling, are too high in the VCI calculations, because at this level of calculation, the charge-transfer states are described with the orbitals of the neutral configurations. The error in the energy of the charge-transfer states can be estimated from calculations on mononuclear clusters. First, the orbitals for the neutral configurations are obtained by state-averaged CASSCF calculations for Mn(III) centers and a self-consistent-field calculation for the Mn(II) center. Next, the energy expectation values of the systems with one additional electron, and with one electron less, are calculated with these orbitals. In the last step, the orbitals are relaxed and the energy difference for unrelaxed and relaxed orbitals is obtained. The relaxation energy for the charge-transfer states in the binuclear complex is then obtained as the sum of the relaxation energies of the two centers (see E_{rel} in Table VII). In the modified CASCI calculations, the charge-transfer states are lowered by the relaxation energy E_{rel} . Because of the lower energy, the weight of the charge-transfer states, and in consequence the super-exchange coupling, is increased in the modified CASCI (MCI) calculations. The resulting coupling constants J_{MCI} are much more reliable than J_{VCI} . For the coupling of two Mn(III) centers, we perform state-averaged CASSCF calculations in the space of the ten $3d$ orbitals for the four lowest high-spin states. Next, we perform CASSCF calculations on the lowest nonet and septet state and obtain natural orbitals for those states. In the ground state, only four of the $3d$ orbitals are occupied at each center. The occupied and unoccupied orbitals are localized individually and the coupling constants

are obtained in the same manner as described above.

The results are summarized in Table VII. For the antiferromagnetic couplings J_{14} , J_{24} , J_{34} , and J_{13} , the agreement between the modified CASCI and the DFT calculation is really excellent. The DFT values are slightly larger than the modified CASCI values, but the deviations are small. The situation is different for the coupling constants J_{12} and J_{23} . While these coupling constants were found to be ferromagnetic in the DFT calculations, they are slightly antiferromagnetic in the modified CASCI calculations. To exclude that this difference is caused by the different cluster models, we calculated the exchange coupling J_{12} at the DFT level for the small cluster. The calculations yielded an even somewhat larger ferromagnetic coupling of $J_{12} = 9.9$ K. So far, the results from the modified CASCI approach show the best agreement with the experimentally obtained values.

C. Magnetic susceptibilities

Based on the calculated coupling constants, temperature dependent magnetic susceptibilities were calculated. A comparison with the experimental measurement is given in Figure 4. Clearly, the geometrical changes between the optimized and XRD structures lead for the optimized and the two-center coupling constants to an upward shift of the χT versus T curves. In contrast, the values that are based on the XRD structure are very close to the experimental values.

The XRD-structure-based curves and the experiment are compared in detail in Figure 5. The agreement between the calculations and the experiment is very good in the range of 14–300 K, but in the low temperature range (1.8–13 K), the susceptibilities that are based on the DFT coupling constants of the tetranuclear cluster show a different behavior from the measured data and are nearly constant. This trend is not seen for the curve that is based on two-center interactions, although the values of the coupling constants are very similar. The deviations range between 0.1 K (J_{34}) and 2.3 K (J_{14}). Thus, the system reacts very sensitive to small changes in the coupling constants. As expected, because the coupling constants are very similar, the curve based on the modified CASCI coupling constants shows the best agreement with the experiment.

Finally, the calculated exchange couplings were taken as start values for a least-squares fitting procedure to experimental magnetic susceptibilities. The results are listed in Ta-

ble VIII. Both DFT starting values lead to almost the same minimum with a maximum absolute deviation of 0.9 K, which is found for J_{14} . Figure 6 shows that a good agreement with experiment is obtained for clearly different coupling constants. The values obtained from the fit should hence be regarded with some care.

Analyzing the energy eigenvalues of the model Heisenberg Hamiltonian allows the determination of the resulting total spin state of the system, which is summarized for all employed quantum chemical models in Table IX. When the total spin state equals $\frac{1}{2}$ then the corresponding coupling constants lead to a correct theoretical description of the overall shape of the experimental χT versus T curve. In particular the correct description of the low temperature range is important, since different total spin states result.

So far, the MCI description of the coupling constants with the two-center interactions seems (from a quantum chemical point of view) to be the best estimate for the exchange coupling constants for the present Mn_4 system. Although being a rough estimate, since the cluster had to be cut into small model systems, it describes the experimental results very well, avoiding a fitting procedure. Furthermore it gives the correct trends and the correct total spin.

V. SUMMARY

In the present work, the magnetic exchange couplings on the mixed valent Photosystem II like model compound of Hewitt *et al.* were investigated at the DFT level, using the broken-symmetry approach. The six coupling constants for the investigated $\text{Mn}^{2+}/\text{Mn}^{3+}$ system were obtained by a fit to the energies of eight Kohn–Sham determinants. The results were compared with pure two-center interactions, created by replacing $\text{Mn}^{2+}/\text{Mn}^{3+}$ with $\text{Mg}^{2+}/\text{Al}^{3+}$ atoms. They were very similar with a maximum deviation of 2.3 K. In all DFT calculations, J_{12} and J_{23} , which were neglected in previous work,[6] were ferromagnetic, whereas they were small and antiferromagnetic in the modified CASCI calculations on smaller model complexes.

Based on the calculated coupling constants, temperature dependent magnetic susceptibilities were calculated and compared with experimental measurements. The susceptibilities based on the full optimized coupling constants show a good agreement with experiment for high temperatures, but differ in the low temperature range. In contrast, the results based

on the pairwise interactions give an overall good agreement with experiment. The results show that even small changes in the coupling constants have drastic consequences for the whole system, such as different total spin states. The best agreement with the measured susceptibilities was observed for the coupling constants obtained with the modified CASCI approach. It seems that the coupling constants for the coupling of two Mn(III) centers by the central oxygen are too ferromagnetic in the broken symmetry DFT approach.

The results for the coupling constants J_{13} , J_{14} , J_{24} , and J_{34} can be regarded as trustworthy, since all calculations show the same trends and are in good agreement with experiment.

VI. ACKNOWLEDGMENT

This research has been supported by the Deutsche Forschungsgemeinschaft through the Center for Functional Nanostructures (CFN, Projects No. C3.3, C1.2 and C3.7). It has been further supported by a grant from the Ministry of Science, Research and the Arts of Baden-Württemberg (Az: 7713.14-300). R.C., A.P. and C.A. thank the European network MAGMANet (NMP3-CT-2005-515767). R.C. thanks the University of Bordeaux, the CNRS and the Région Aquitaine for financial support. H.F. and K.F. thank Prof. Dr. Staemmler for providing a copy of a Fortran program concerning magnetic susceptibilities.

-
- [1] V. K. Yachandra in *Photosystem II, The Light-Driven Water: Plastoquinone Oxidoreductase*; ed. by T. J. Wydrzynski and K. Satoh, vol. 22 of "Advances in Photosynthesis and Respiration", Springer, 2005; p. 235.
- [2] B. Kok, B. Forbush, and M. McGloin, *Photochem. Photobiol.*, 1970, **11**, 457.
- [3] K. N. Ferreira, T. M. Iverson, K. Maghlaoui, J. Barber, and S. Iwata, *Science*, 2004, **303**, 1831.
- [4] B. Loll, J. Kern, W. Saenger, A. Zouni, and J. Biesiadka, *Nature*, 2005, **438**, 1040.
- [5] J. Yano, J. Kern, K. Sauer, M. J. Latimer, Y. Pushkar, J. Biesiadka, B. Loll, W. Saenger, J. Messinger, A. Zouni, and V. K. Yachandra, *Science*, 2006, **314**, 821.
- [6] I. J. Hewitt, J. Tang, N. T. Madhu, R. Clérac, G. Buth, C. E. Anson, and A. K. Powell, *Chem. Commun.*, 2006, p. 2650.
- [7] J. Messinger, J. H. Robblee, W. O. Yu, K. Sauer, V. K. Yachandra, and M. P. Klein, *J. Am. Chem. Soc.*, 1997, **119**, 11349.
- [8] C. Angeli, A. Cavallini, and R. Cimiraglia, *J. Chem. Phys.*, 2008, **128**, 244317.
- [9] F. Illas, I. de P. R. Moreira, C. de Graaf, O. Castell, and J. Casanovas, *Phys. Rev. B*, 1997, **56**, 5069.
- [10] L. Noodleman, *J. Chem. Phys.*, 1981, **74**(10), 5737.
- [11] L. Noodleman and D. A. Chase in *Advances in Inorganic Chemistry*; Academic Press Inc., 1992; p. 423.
- [12] E. Ruiz, T. Cauchy, J. Cano, R. Costa, J. Tercero, and S. Alvarez, *J. Am. Chem. Soc.*, 2008, **130**, 7420.
- [13] O. Kahn, *Molecular Magnetism*, VCH New York, Weinheim, 1993.
- [14] F. Illas, I. de P. R. Moreira, J. M. Bofill, and M. Filatov, *Theor. Chem. Acc.*, 2006, **116**, 587.
- [15] R. Caballol, O. Castell, F. Illas, I. de P. R. Moreira, and J. P. Malrieu, *J. Phys. Chem.*, 1997, **101**, 7860.
- [16] I. Rudra, Q. Wu, and T. Van Voorhis, *J. Chem. Phys.*, 2006, **124**, 024103.
- [17] I. Rudra, Q. Wu, and T. Van Voorhis, *Inorg. Chem.*, 2007, **46**, 10539.
- [18] K. Fink, C. Wang, and V. Staemmler, *Inorg. Chem.*, 1999, **38**, 3847.
- [19] K. Fink, *Chem. Phys.*, 2006, **326**, 297.

- [20] F. Illas, I. de P. R. Moreira, C. de Graaf, and V. Barone, *Theor. Chem. Acc.*, 2000, **104**, 265.
- [21] I. de P. R. Moreira and F. Illas, *Phys. Chem. Chem. Phys.*, 2006, **8**, 1645.
- [22] W. H. Press, S. A. Teukolsky, W. T. Vetterling, and B. P. Flannery, *Numerical Recipes in Fortran: The Art of Scientific Computing, Second Edition*, Cambridge University Press, 1992.
- [23] J.-M. Mouesca, J. L. Chen, L. Noodleman, D. Bashford, and D. A. Case, *J. Am. Chem. Soc.*, 1994, **116**, 11898.
- [24] S. Sinnecker, F. Neese, L. Noodleman, and W. Lubitz, *J. Am. Chem. Soc.*, 2004, **126**, 2613.
- [25] K. Eichkorn, O. Treutler, H. Öhm, M. Häser, and R. Ahlrichs, *Chem. Phys. Lett.*, 1995, **240**, 283.
- [26] A. D. Becke, *Phys. Rev. A*, 1988, **38**, 3098.
- [27] P. Perdew, *Phys. Rev. B*, 1986, **33**, 8822.
- [28] F. Weigend and R. Ahlrichs, *Phys. Chem. Chem. Phys.*, 2005, **7**, 3297.
- [29] C. Lee, W. Yang, and R. G. Parr, *Phys. Rev. B*, 1988, **37**, 785.
- [30] L. R. Martin and F. Illas, *Phys. Rev. Lett.*, 1997, **79**, 1539.
- [31] F. A. Bischoff, O. Hübner, W. Klopper, L. Schnelzer, B. Pilawa, M. Horvatić, and C. Berthier, *Eur. Phys. J. B*, 2007, **55**, 229.
- [32] O. Hübner, K. Fink, and W. Klopper, *Phys. Chem. Chem. Phys.*, 2007, **9**, 1911.
- [33] E. Ruiz, P. Alemany, S. Alvarez, and J. Cano, *J. Am. Chem. Soc.*, 1997, **119**, 1297.
- [34] H. Nieber, K. Doll, and G. Zwicknagl, *Eur. Phys. J. B*, 2006, **51**, 215.
- [35] J. L. Whitten, *J. Chem. Phys.*, 1973, **58**, 4496.
- [36] B. I. Dunlap, J. W. D. Conolly, and R. Sabin, *J. Chem. Phys.*, 1979, **71**, 3396.
- [37] O. Vahtras, J. Almlöf, and M. W. Feyereisen, *Chem. Phys. Lett.*, 1993, **213**, 514.
- [38] V. Staemmler, *personal communication*, 2007.
- [39] P. Chaudhuri, F. Birkelbach, M. Winter, V. Staemmler, P. Fleischhauer, W. Hasse, U. Flörke, and H.-J. Haupt, *J. Chem. Soc. Dalton Trans.*, 1994, p. 2313.
- [40] V. Staemmler, *Theoret. Chim. Acta*, 1977, **45**, 89.
- [41] U. Meier and V. Staemmler, *Theoret. Chim. Acta*, 1989, **76**, 95.
- [42] S. Huzinaga, *Approximate Atomic Functions. I*. University of Alberta, Canada, 1971.
- [43] A. Wachters, *J. Chem. Phys.*, 1970, **52**, 1033.
- [44] J. M. Foster and S. F. Boys, *Rev. Mod. Phys.*, 1960, **32**, 300.

TABLE I: High-spin state and broken symmetry spin states of the investigated Mn_4 complex ($S_1 = S_2 = S_3 = 2, S_4 = \frac{5}{2}$) and corresponding total Ising energies.

spin state	S_1	S_2	S_3	S_4	energy
Φ_1^{HS}	α	α	α	α	$E_1^{\text{HS}} = -2[4J_{12} + 4J_{13} + 5J_{14} + 4J_{23} + 5J_{24} + 5J_{34}]$
Φ_2^{BS}	α	α	α	β	$E_2^{\text{BS}} = -2[4J_{12} + 4J_{13} - 5J_{14} + 4J_{23} - 5J_{24} - 5J_{34}]$
Φ_3^{BS}	α	α	β	α	$E_3^{\text{BS}} = -2[4J_{12} - 4J_{13} + 5J_{14} - 4J_{23} + 5J_{24} - 5J_{34}]$
Φ_4^{BS}	α	β	α	α	$E_4^{\text{BS}} = -2[-4J_{12} + 4J_{13} + 5J_{14} - 4J_{23} - 5J_{24} + 5J_{34}]$
Φ_5^{BS}	β	α	α	α	$E_5^{\text{BS}} = -2[-4J_{12} - 4J_{13} - 5J_{14} + 4J_{23} + 5J_{24} + 5J_{34}]$
Φ_6^{BS}	α	α	β	β	$E_6^{\text{BS}} = -2[4J_{12} - 4J_{13} - 5J_{14} - 4J_{23} - 5J_{24} + 5J_{34}]$
Φ_7^{BS}	α	β	α	β	$E_7^{\text{BS}} = -2[-4J_{12} + 4J_{13} - 5J_{14} - 4J_{23} + 5J_{24} - 5J_{34}]$
Φ_8^{BS}	α	β	β	α	$E_8^{\text{BS}} = -2[-4J_{12} - 4J_{13} + 5J_{14} + 4J_{23} - 5J_{24} - 5J_{34}]$

TABLE II: Calculated BP86/def2-TZVP Mn-Mn distances in pm and angles in $^\circ$ in comparison to XRD data[6].

	BP86	XRD		BP86	XRD
Mn ₁ -Mn ₂	336.4	327.3	\angle Mn ₁ -Mn ₂ -Mn ₃	63.5	63.1
Mn ₁ -Mn ₃	348.3	339.9	\angle Mn ₁ -Mn ₂ -Mn ₄	63.5	63.1
Mn ₁ -Mn ₄	355.3	351.3	\angle Mn ₁ -Mn ₃ -Mn ₄	61.5	60.9
Mn ₂ -Mn ₃	325.4	322.6	\angle Mn ₂ -Mn ₃ -Mn ₄	60.4	61.0
Mn ₂ -Mn ₄	338.8	343.9			
Mn ₃ -Mn ₄	347.1	353.4			

TABLE III: Selected calculated BP86/def2-TZVP bond distances in pm and angles in degrees in comparison with XRD data.[6]

	BP86	XRD		BP86	XRD
Mn ₁ -O ₉	194.8	191.0	Mn ₃ -O ₈₈	194.2	191.2
Mn ₁ -O ₁₀	190.9	187.5	Mn ₃ -O ₆₆	190.7	187.3
Mn ₁ -O ₃₂	197.9	194.4	Mn ₃ -O ₉₅	237.5	221.8
Mn ₁ -O ₉₄	216.7	214.8	Mn ₃ -O ₉	195.3	190.5
Mn ₁ -N ₂₀	198.7	197.3	Mn ₃ -N ₇₆	197.4	197.1
Mn ₁ -Cl ₆	283.5	279.2	Mn ₃ -Cl ₇	255.5	266.1
Mn ₂ -O ₆₀	194.8	193.0	Mn ₄ -O ₈₈	223.4	216.8
Mn ₂ -O ₃₈	191.8	192.1	Mn ₄ -O ₈₉	265.8	238.3
Mn ₂ -O ₉	197.2	193.1	Mn ₄ -O ₃₂	229.8	224.3
Mn ₂ -Cl ₆	264.6	257.0	Mn ₄ -O ₃₃	238.0	225.7
Mn ₂ -Cl ₇	258.0	258.5	Mn ₄ -O ₃₈	215.0	212.3
Mn ₂ -N ₄₈	198.6	195.9	Mn ₄ -Cl ₈	229.4	244.3
∠ O ₃₂ -Mn ₁ -N ₂₀	90.14	60.97	∠ Mn ₂ -O ₃₈ -Mn ₄	112.69	116.46
∠ N ₂₀ -Mn ₁ -O ₁₀	82.80	89.34	∠ Mn ₂ -O ₃₈ -C ₃₉	112.04	113.53
∠ O ₉ -Mn ₁ -O ₁₀	90.82	84.79	∠ Mn ₂ -O ₉ -Mn ₁	118.20	116.88
∠ O ₉ -Mn ₁ -O ₃₂	95.50	89.33	∠ Mn ₂ -O ₉ -Mn ₃	112.04	114.48
∠ Mn ₁ -O ₉ -Mn ₃	126.45	96.15	∠ Mn ₃ -O ₉ -Mn ₁	126.45	125.94
∠ Mn ₁ -O ₉ -Mn ₂	118.20	125.94	∠ O ₆₆ -Mn ₃ -O ₉₅	81.76	90.09
∠ Mn ₁ -O ₃₂ -Mn ₄	112.09	116.88	∠ O ₆₆ -Mn ₃ -O ₈₈	172.04	174.81
∠ Mn ₁ -Cl ₆ -Mn ₂	75.63	113.89	∠ O ₃₃ -Mn ₄ -O ₈₈	142.41	151.85
∠ O ₆₀ -Mn ₂ -Cl ₆	88.40	75.12	∠ Cl ₈ -Mn ₄ -O ₃₃	90.28	93.77
∠ O ₃₈ -Mn ₂ -Cl ₆	93.66	89.92	∠ Cl ₈ -Mn ₄ -O ₃₈	105.31	104.07
∠ Cl ₆ -Mn ₂ -O ₉	82.30	92.67	∠ Mn ₄ -O ₃₈ -Mn ₂	112.69	116.46
∠ O ₆₀ -Mn ₂ -N ₄₈	88.72	84.63	∠ O ₃₂ -Mn ₄ -O ₈₈	96.47	100.19
∠ Mn ₄ -O ₈₈ -Mn ₃	112.26	119.90			

TABLE IV: CASSCF calculations on mononuclear Mn^{3+} clusters: Relative energies of the five quintet states in eV.

state	Mn ₁	Mn ₂	Mn ₃
1	0.0	0.0	0.0
2	1.56	1.48	1.93
3	2.30	2.42	2.42
4	2.62	2.70	2.79
5	2.93	2.93	3.17

TABLE V: Calculated B3LYP/def2-TZVP magnetic spin-coupling constants (in K) in comparison with experimental results.[6]

	B3LYP ^a	B3LYP ^b	Exp.
J ₁₂	5.6	6.8	0
J ₁₃	-7.6	-13.7	-10
J ₁₄	-4.1	-7.2	-5
J ₂₃	11.3	9.7	0
J ₂₄	-7.7	-7.5	-5
J ₃₄	-4.2	-5.7	-5

^a The geometry was optimized at the BP86/def2-TZVP level.

^b Results are based on the XRD geometry.

TABLE VI: Calculated B3LYP/def2-TZVP magnetic spin-coupling constants (in K) in comparison with experimental results.[6] The not directly neighboring manganese atoms are replaced by Al^{+3} and Mg^{+2} atoms.

	B3LYP ^a	B3LYP ^b	Exp.
J_{12}	5.5	6.2	0
J_{13}	-8.4	-15.2	-10
J_{14}	-2.3	-4.9	-5
J_{23}	11.1	9.1	0
J_{24}	-7.9	-7.2	-5
J_{34}	-4.0	-5.8	-5

^a The geometry was optimized on BP86/def2-TZVP level.

^b Results are based on the XRD geometry.

TABLE VII: Coupling constants J_{ij} in K obtained with the modified CASCI method.

Coupling	E_{rel}	J_{VCI}	J_f	J_{MCI}
J_{12}	13.31	3.3	6.3	-1.2
J_{13}	13.16	-0.7	6.2	-10.9
J_{14}	11.04	-1.0	1.9	-4.1
J_{23}	12.21	4.3	7.0	-1.7
J_{24}	10.69	-2.2	4.3	-5.7
J_{34}	10.54	-1.6	3.4	-5.4

TABLE VIII: Fitted magnetic spin-coupling constants (in K) in comparison with experimental results.[6]

	Fit ^a	Fit ^b	Fit ^c	Exp.
J_{12}	6.1	5.9	-0.3	0
J_{13}	-14.6	-14.6	-9.6	-10
J_{14}	-4.5	-3.6	-3.7	-5
J_{23}	9.1	9.0	-1.7	0
J_{24}	-7.0	-6.7	-5.1	-5
J_{34}	-4.2	-4.5	-5.0	-5

^a Based on the DFT coupling constants for the tetranuclear cluster.

^b Based on the DFT coupling constants for the pair interactions.

^c Based on the modified CASCI coupling constants.

TABLE IX: Overview of the calculated total spin states.

structure	determination of J	total spin state
XRD	DFT 4 center interaction	$\frac{3}{2}$
XRD	DFT 2 center interaction	$\frac{1}{2}$
XRD	MCI 2 center interaction	$\frac{1}{2}$
optimized DFT	4 center interaction	$\frac{5}{2}$
optimized DFT	2 center interaction	$\frac{3}{2}$

- Fig. 1** Structure of the investigated molecule.(color code: black (C), grey (H), pink (Mn), yellow (Ca), green (Cl), blue (N), red (O)).
- Fig. 2** Assignment of the coupling constants according to Ref.6. (a) The coupling over the central oxygen atom was considered to be negligible. Thus, J_{12} and J_{23} were set to zero and the coupling between similarly bridged centers was considered to be identical. (b) The coupling between the Mn centers 1 and 3 over the CH_3COO^- group was considered to be large and antiferromagnetic.
- Fig. 3** Structure of the Mn_3 model system.
- Fig. 4** Calculated magnetic susceptibilities for different exchange coupling constants in comparison with experimental data and with the previous fit of Ref. 6. The structure used is indicated in parenthesis.
- Fig. 5** Calculated magnetic susceptibilities for different exchange coupling constants, which are all based on the XRD structure, in comparison with experimental data and with the previous fit of Ref. 6.
- Fig. 6** Calculated magnetic susceptibilities for different exchange coupling constants, which are all based on the XRD structure, in comparison with the experimental data.[6] The curves refer to the fitted values of Table VIII.

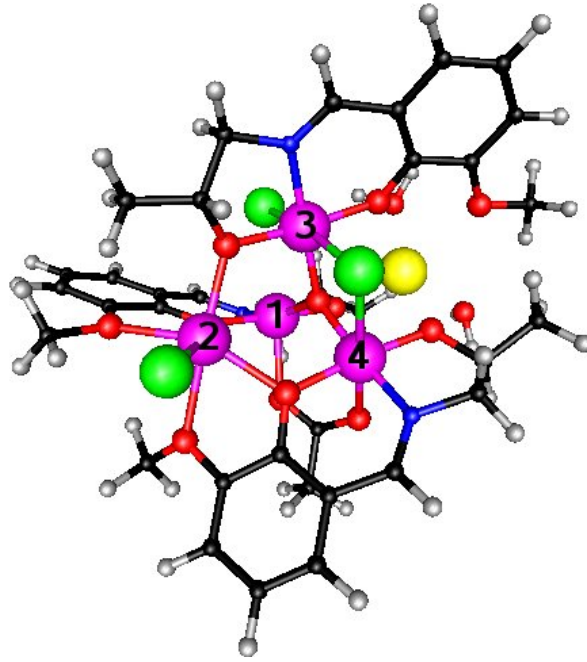
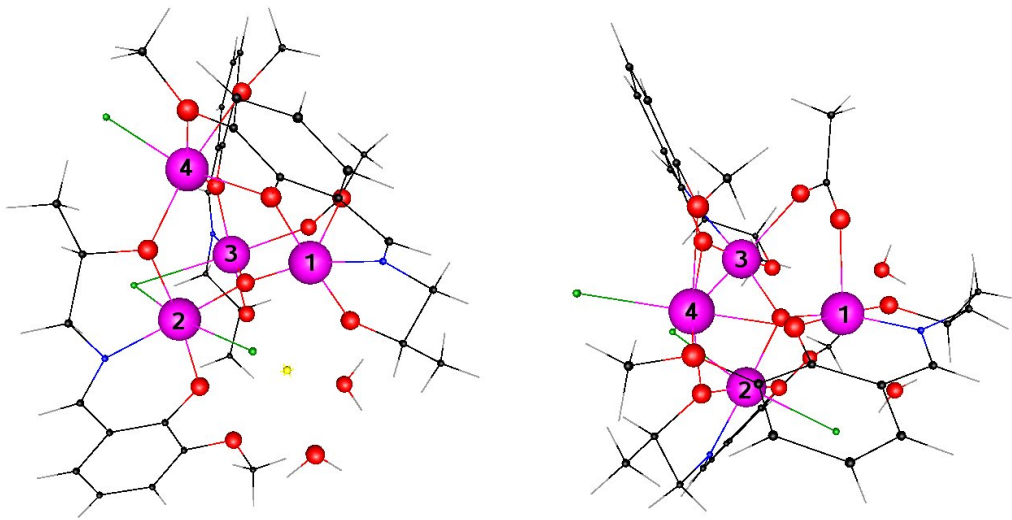


FIG. 1: Structure of the investigated molecule.(color code: black (C), grey (H), pink (Mn), yellow (Ca), green (Cl), blue (N), red (O))



(a) $J_{12} = J_{23} = 0, J_{14} = J_{24} = J_{34}$

(b) $J_{13} < 0$

FIG. 2: Assignment of the coupling constants according to Ref.6. (a) The coupling over the central oxygen atom was considered to be negligible. Thus, J_{12} and J_{23} were set to zero and the coupling between similarly bridged centers was considered to be identical. (b) The coupling between the Mn centers 1 and 3 over the CH_3COO^- group was considered to be large and antiferromagnetic.

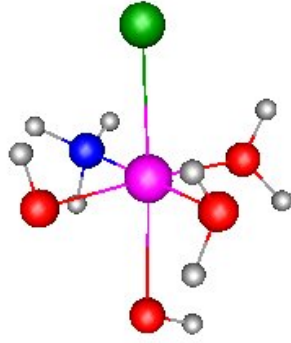


FIG. 3: Structure of the Mn_3 model system.

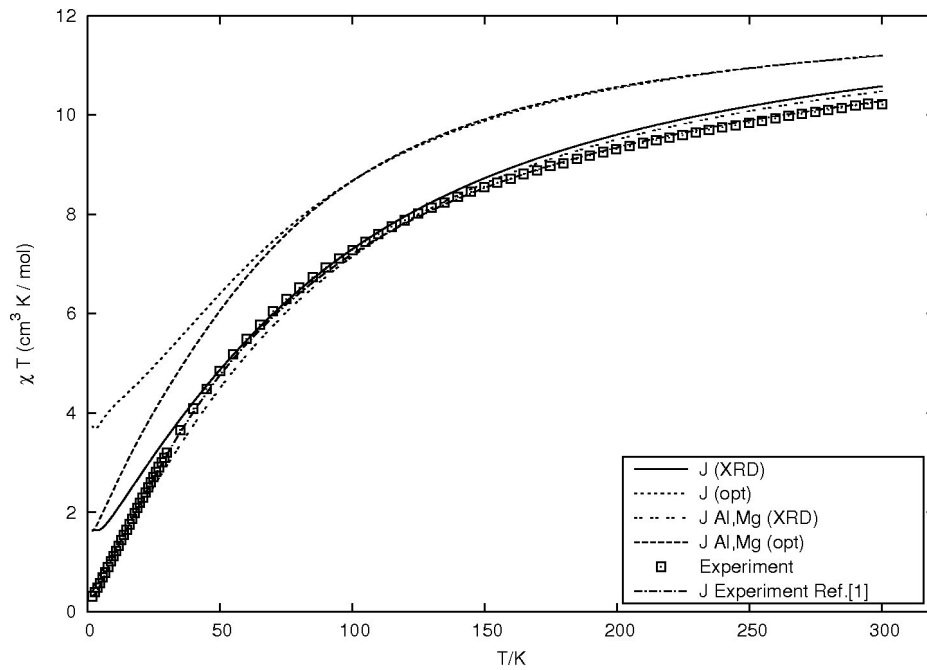
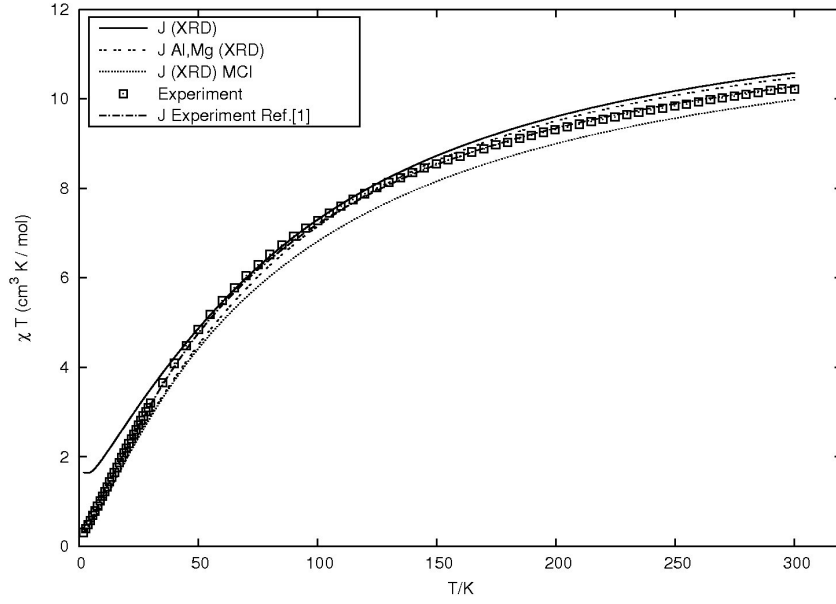
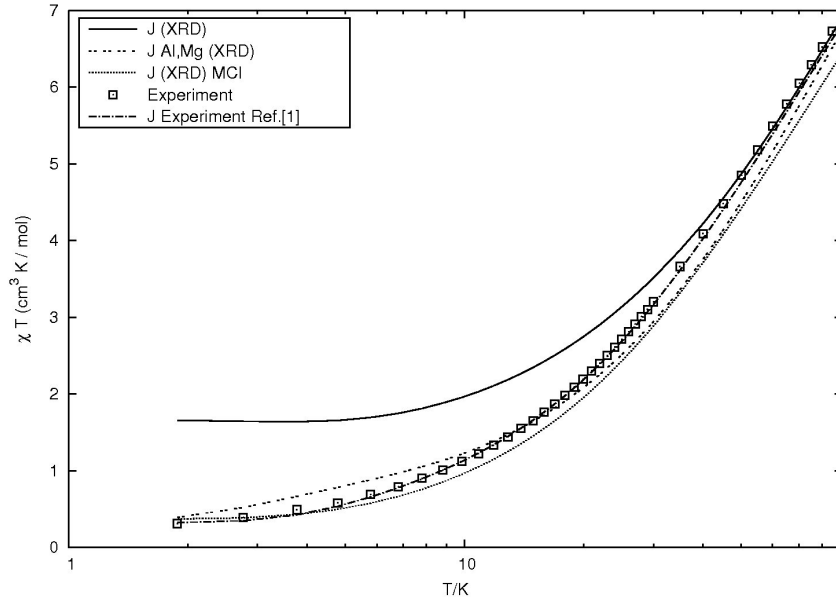


FIG. 4: Calculated magnetic susceptibilities for different exchange coupling constants in comparison with experimental data and with the previous fit of Ref. 6. The structure used is indicated in parenthesis.

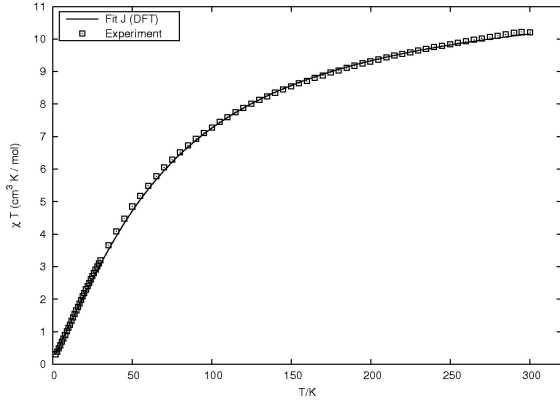


(a)

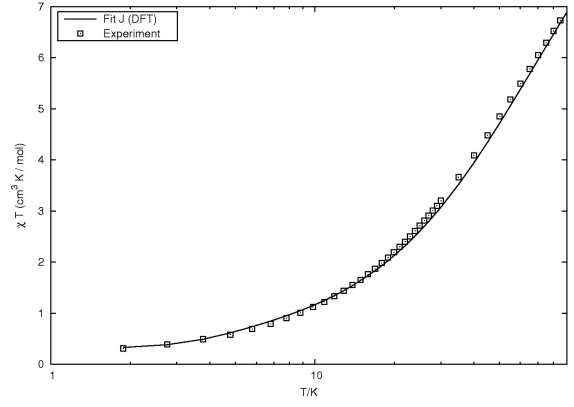


(b)

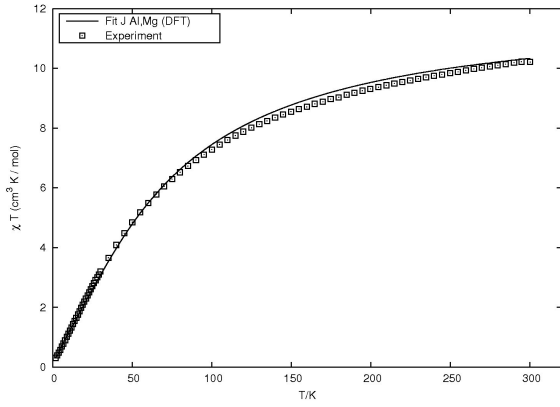
FIG. 5: Calculated magnetic susceptibilities for different exchange coupling constants, which are all based on the XRD structure, in comparison with experimental data and with the previous fit of Ref. 6.



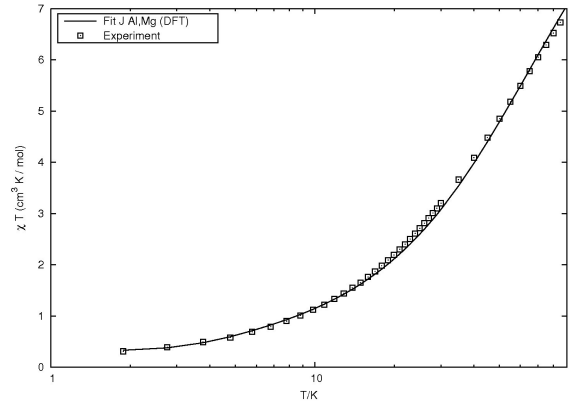
(a)



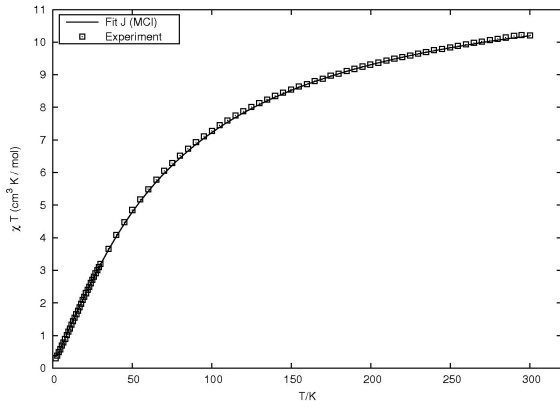
(b)



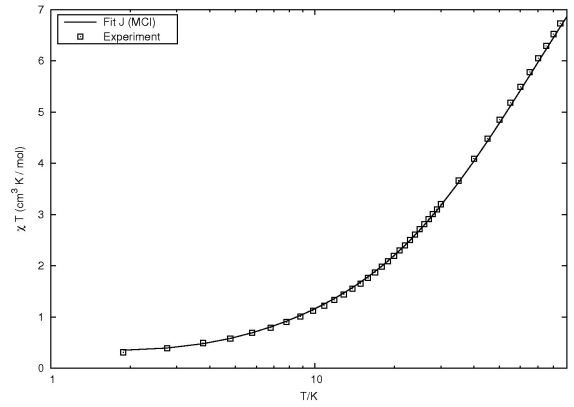
(c)



(d)



(e)



(f)

FIG. 6: Calculated magnetic susceptibilities for different exchange coupling constants, which are all based on the XRD structure, in comparison with the experimental data.[6] The curves refer to the fitted values of Table VIII.